RGNZ/MGPB

Computational Simulation of Sediment Motion Stability Process on Bridge Abutment Due to Crib Placement (Case Study: Harapan River, Jayapura Regency)

Rudarsko-geološko-naftni zbornik
(The Mining-Geology-Petroleum Engineering Bulletin)
UDC: 627.28
DOI: 10.17794/rgn.2024.4.6

Original scientific paper

Ira Widyastuti[1], Mujiati[2], Davy Ivan Robert Jansen[3], Ahmad Fauzi Yunus[4]

[1] *Department of Civil Engineering, University of Cenderawasih, Papua, Indonesia, ORCID https://orcid.org/0009-0008-2099-7123*

[2] *Department of Civil Engineering, University of Cenderawasih, Papua, Indonesia, ORCID https://orchid.org/0009-0007-8339-754X*

[3] *Department of Civil Engineering, University of Cenderawasih, Papua, Indonesia, ORCID https://orcid.org/0009-0008-1394-8649*

[4] *Research Center for Geological Disaster, National Research, and Innovation Agency (BRIN), Bandung, Indonesia, ORCID https://orcid.org/0009-0005-6673-1943*

Abstract

Erosion occurs when the flow of velocity in a channel exceeds the threshold velocity that causes the bed material to move. This phenomenon is observed in the Harapan River, resulting in significant impacts, such as riverbed lowering and narrowing due to the presence of water structures (bridge abutments) spanning across the river. The objective of this study is to investigate the sediment motion stability around bridge abutments before and after the installation of cribs in order to prevent structural failures. Sediment sampling was conducted at six points around the bridge abutments, using the *Pebble Count* method along *zigzag* paths. The grain size of the bed material was classified according to the Sturgess classification standard, and the material dispersion process was analysed using the Hjustorm curve. Design rainfall was transformed into design flood discharge, which was then simulated using the *Two-Dimensional Hydrodynamic*, comparing the river conditions before and after crib installation. In abutments without cribs, erosion occurred in direct contact with the abutment on the right side for each sediment grain diameter. However, in abutments with cribs, erosion still occurred, but it did not directly contact either abutment despite the presence of a crib. The crib prevented and protected the abutments from being eroded by the riverbed.

Keywords:
computational simulation; crib; Harapan River; sediment motion stability

1. Introduction

Local erosion on bridge abutments and piers is a significant issue within the hydraulic research community due to its social and economic impacts. Experimental and numerical studies on erosion processes provide support for interpreting their dynamics. Several parameters can influence investigations into abutment erosion. Some researchers have demonstrated the consistency of erosion by utilizing easily erodible abutment embankments (**Hong et al., 2015**). Additionally, the length and shape of the abutment have an impact on the depth and width of erosion (**Abdelaziz and Lim, 2017; Radice et al., 2009**). **Figure 1** illustrates that the positioning of abutments in river bend regions has the potential to undergo structural failure as a result of ongoing scouring.

Furthermore, the addition of elements on the abutment wall reduces the depth of erosion on the abutment (**Ballio et al., 2010; Shahsavari et al., 2017**). Research depicting flow patterns resulting from obstructions has also been conducted (**Ballio et al., 2009; Koken and Constantinescu, 2014; Armenio, 2017**). The decrease in channel bed elevation is known as local scour (**Radice and Davari, 2014**). Downstream (sideways) of the abutment, the flow velocity tends to be slower and swirling (*vortex*). Still, the energy generated is not significant, resulting in localized scour and subsequent aggradation around the abutment (**Widyastuti et al., 2022**).

In meandering rivers, some areas are degraded and aggraded. Suppose the incoming solid discharge is smaller than the sediment transport capacity. In that case, the river will experience a decrease in the riverbed (degradation). At the same time, if the incoming solid discharge is greater than the sediment transport capacity, the riverbed will increase (aggradation). The river flow and the general conditions of erosion and deposition are shown in **Figure 2**.

The bridge abutment on the Harapan River is located in the river bend area and causes scour in the turn area to expand, and flow vortices occur around the abutment so that the riverbed will drop. The interaction effect between abutments and water flow represents a local disturbance in the flow. It will result in flow acceleration through the bridge abutments and increased turbulence, leading to a decrease in the channel bed elevation, which can potentially lead to structural failure of the bridge in the river due to the potential for scour to expand in the river bend area and affect the abutment structure. This study will provide the information and simulation about crib installation.

The Harapan Watershed is a sub-watershed within the Sentani region. The Harapan watershed covers an area

Corresponding author: Widyastuti Ira
e-mail address: iwidyastuti09@gmail.com

Figure 1: Failure of the bridge abutment structure on the Harapan River

Figure 2: Normal flow of Harapan River

of approximately 28.270 square kilometers and extends for a distance of 9.00 kilometers. It is precisely located at coordinates 452260 meters east and 450690 meters south (see **Figure 3**). The predominant land use consists of trees and bushes, which are characterized by seasonal river features. Physiographically, the Harapan watershed is located in a series of Cyclop hills with a height of 80 Masl to 1725 Masl. Genetically, the Harapan Watershed was formed through uplift and has undergone a denudation process. There are several fault and fold geological formations with loose sedimentary formations such as limestone, gravel, sand and silt. The FAO soil database shows that the Harapan watershed has podzolic and latasol type soils.

2. Methodology

River measurements and sediment sampling were conducted along a 1.00 km stretch from the upstream of the abutments using the *pebble* count method. Based on the Wentworth Scale, sediments can be categorized based on their grain size, namely clay, silt, sand, gravel, coral (pebble), cobble, and stone (boulder). The scale shows the standard size of sediment classes from micron-sized fractions to several mm with a continuous spectrum. For the pebble count method, the aggregate boundary condition is that the grain size of coarse gravel ranges from dia ±16 mm to small pebbles dia ±72 mm with a *zigzag* pattern, divided into five sampling points.

2.1. River hydrology

A watershed system is a hydrological system that operates independently. The hydrological process is driven by a primary source and results in multiple kinds of output. Rainwater is the primary source utilized in this investigation. One commonly performed hydrological analysis is the estimation of maximum flood events, particularly for water source planning and flood management, which rely on the frequency and magnitude of peak flow discharge.

The design flood discharge can be calculated using the synthetic unit hydrograph method, specifically the Nakayasu method. The Synthetic Unit Hydrograph (SUH) based on the Nakayasu method is utilized to estimate the potential flood discharge (see **Figure 4**). It is achieved through the Rainfall-Runoff Model analysis using the Nakayasu method (**Choi et al., 1999**). The parameters of the Nakayasu HSS are provided in the following equations:

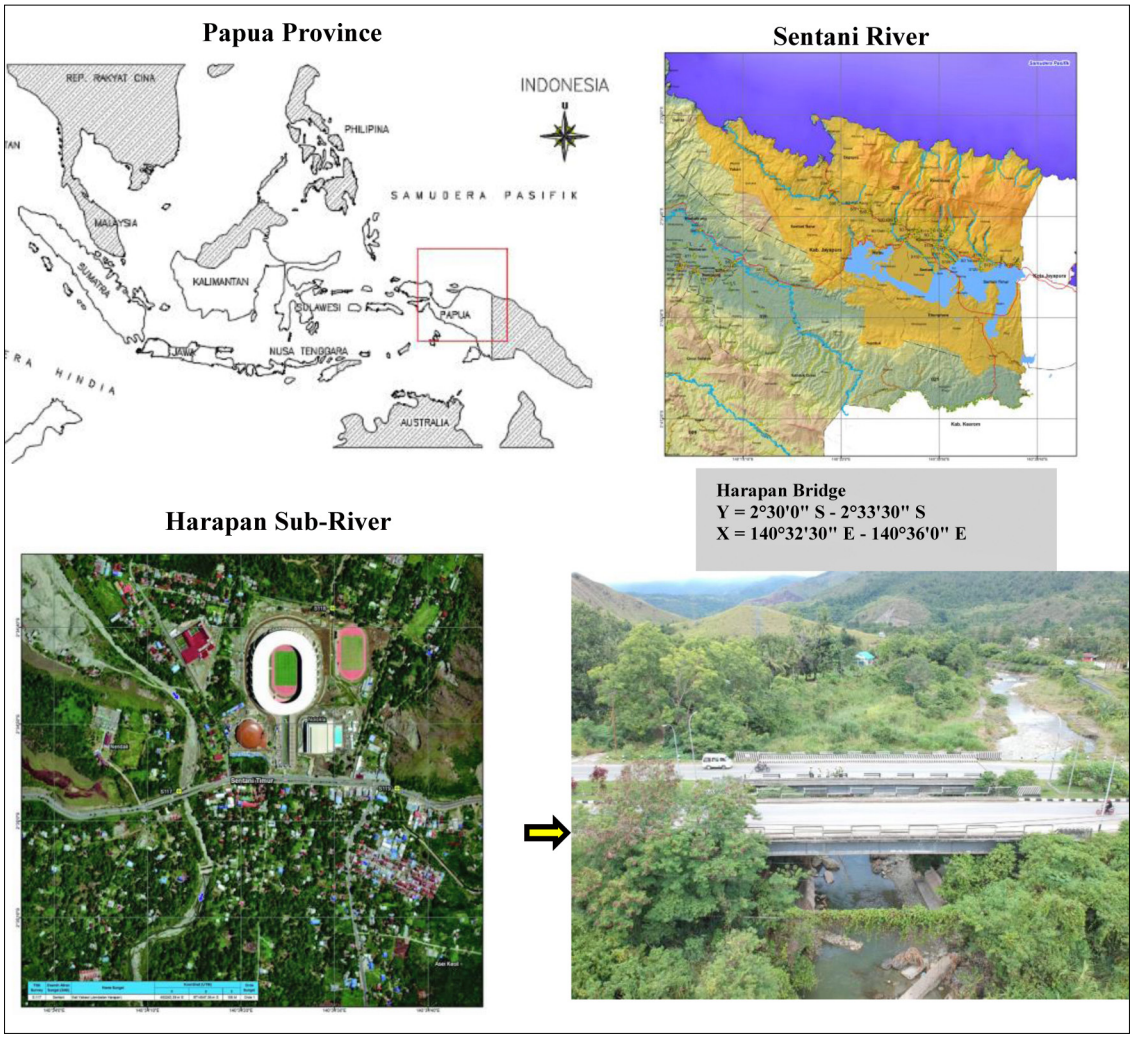

Figure 3: Location of bridge abutment, Papua-Jayapura Regency, Indonesia

$$Q_p = \frac{1}{3.6}\left(\frac{A \cdot R_e}{0.3t_p + t_{0.3}}\right) \quad (1)$$

$$t_p = t_q + 0.8t_r \quad (2)$$

For river lengths exceeding 15 km, the following value:

$$t_q = 0.4 + 0.058 \cdot L \quad (3)$$

For river lengths less than 15 km, the following value:

$t_q = 0.21 + L^{0.7}$

$t_{0.3} = \alpha \cdot t_q$

α = between 1.5 to 3

Where:

Q_p = peak flood discharge (m³/second),
A = watershed area (km²),
R_e = effective rainfall (mm),
t_p = time from the start of the flood until the peak of the flood hydrograph (mm),
$t_{0.3}$ = time from the peak of the flood to 0.3 times the peak flood discharge (hours),
t_g = concentration time,
α = characteristic coefficient of the watershed,
t_r = time unit of rainfall (mm),
L = main river length (km).

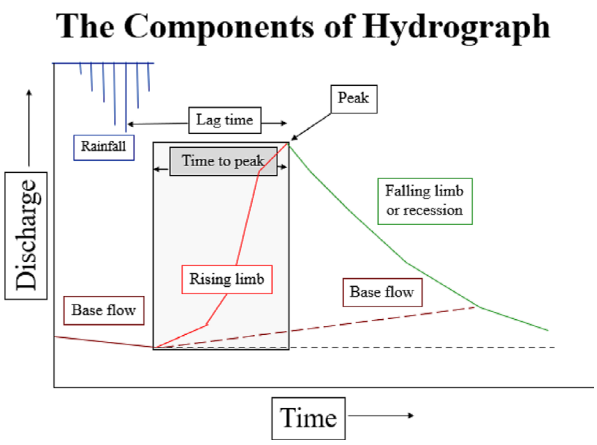

Figure 4: Element of flood hydrograph

2.2. Characteristics and initial motion of sediment grains

The bed material significantly influences the resistance of a river channel to the hydraulic forces that can erode the river. The larger the size of the sediment grains, the greater the river's resistance to erosion. The size of sediment grains is one of the most important characteristics and is widely used in sediment transport equations (**Nelson et al., 2003**). Due to the flow of water, forces act on the sediment grains. When the forces acting on the sediment grains reach a certain threshold, adding a small amount of force will cause the sediment grains to move. This condition is referred to as the critical condition. Flow parameters, such as shear stress (τ_0) and flow velocity (U), also reach critical conditions. Therefore, the shield number can be calculated.

$$\theta_c = \frac{\tau_c}{\rho_w g d} = \frac{U_{ic}^2}{g \Delta d} \quad (4)$$

with: $\rho_{r,i} = \frac{\rho_s - \rho_w}{\rho_w}$¿

Where:

θ_c = shield coef.,
τ_c = shear stress (N/m^2),
ρ_s = specific gravity of sediment (kg/m^3),
ρ_w = specific gravity of water (1000 kg/m^3),
g = gravity (m/det^2),
U_{ic} = the critical shear velocity (m/s),
d = the diameter of the sediment grains (mm),
h = depth (m),
$\rho_{r,i}$ = relative mass density of submerged grains.

The sediment transport rate that occurs is usually in equilibrium condition. Whether it is erosion or deposition, the quantity of sediment transported in the process can be determined (see **Table 1**).

Table 1: Bed sediment processes

The comparison of T	Processes that occur	
	Sediment	Sediment Bed
$t_1 = t_2$	Balanced	Stable
$t_1 < t_2$	Erosion	Degradation
$t_1 > t_2$	Deposition	Aggradation

The Hjulstrom curve is an analysis that can be used to understand the erosion process in a river. This curve indicates the erosion velocity at a specific cross-section, which is the minimum velocity required for a river flow to transport grains of a certain size on the riverbed (**Geier, 1996**). Lower erosion velocities are capable of transporting sand-sized grains more effectively compared to silt or gravel-sized grains. The Hjulstrom diagram consists of two dividing curves (see **Figure 5**).

The upper blue curve represents the erosion velocity (this curve is above the entrainment velocity) in centimeters per second as a function of grain size in millimeters. In contrast, the lower cream curve represents the settling velocity as a function of grain size, indicating the speed at which grains settle (**Lerche, 2019**). Between the erosion and sedimentation curves, there is a gray-colored transitional zone where grains neither undergo erosion nor sedimentation but remain in transport within a medium.

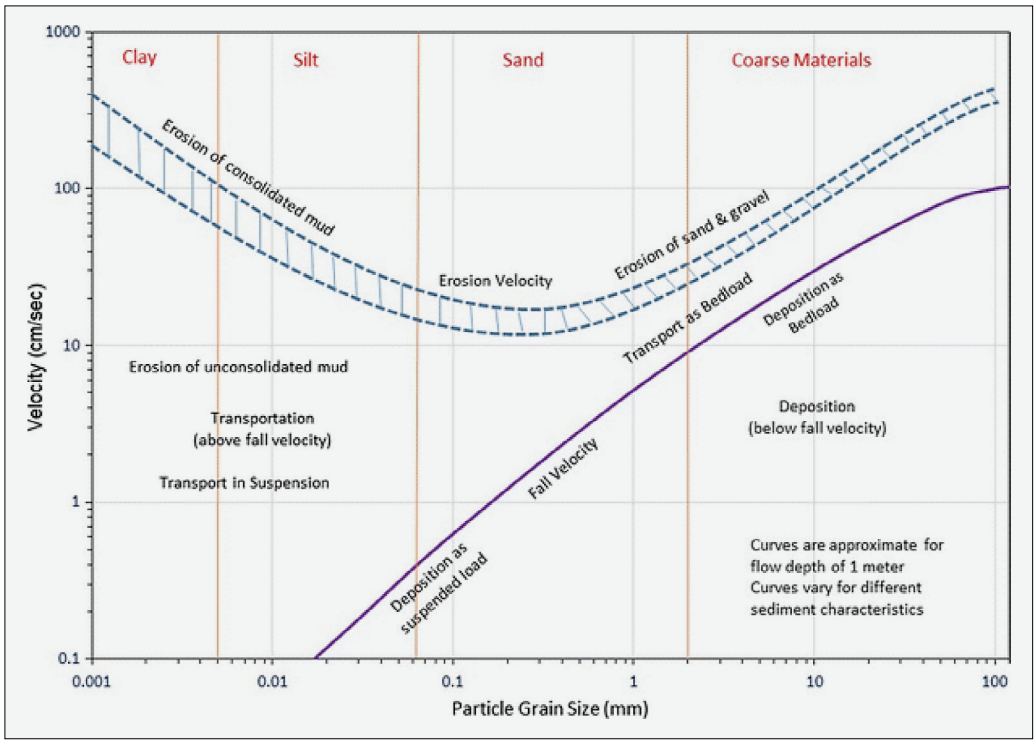

Figure 5: Hujulstrom Diagram

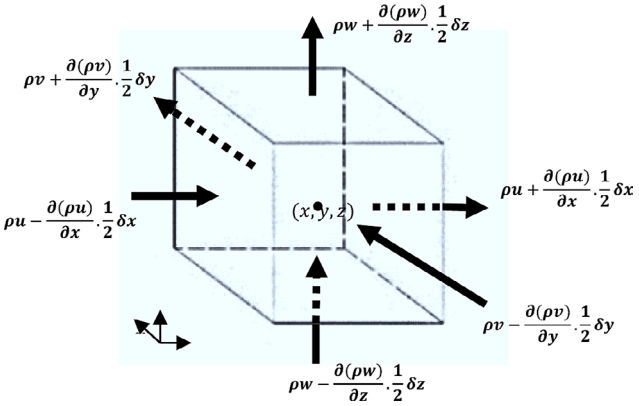

Figure 6: The direction of mass flow in the fluid element

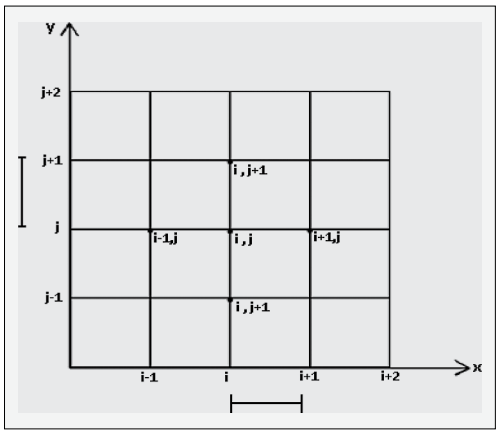

Figure 7: Grid point layout in x and y directions

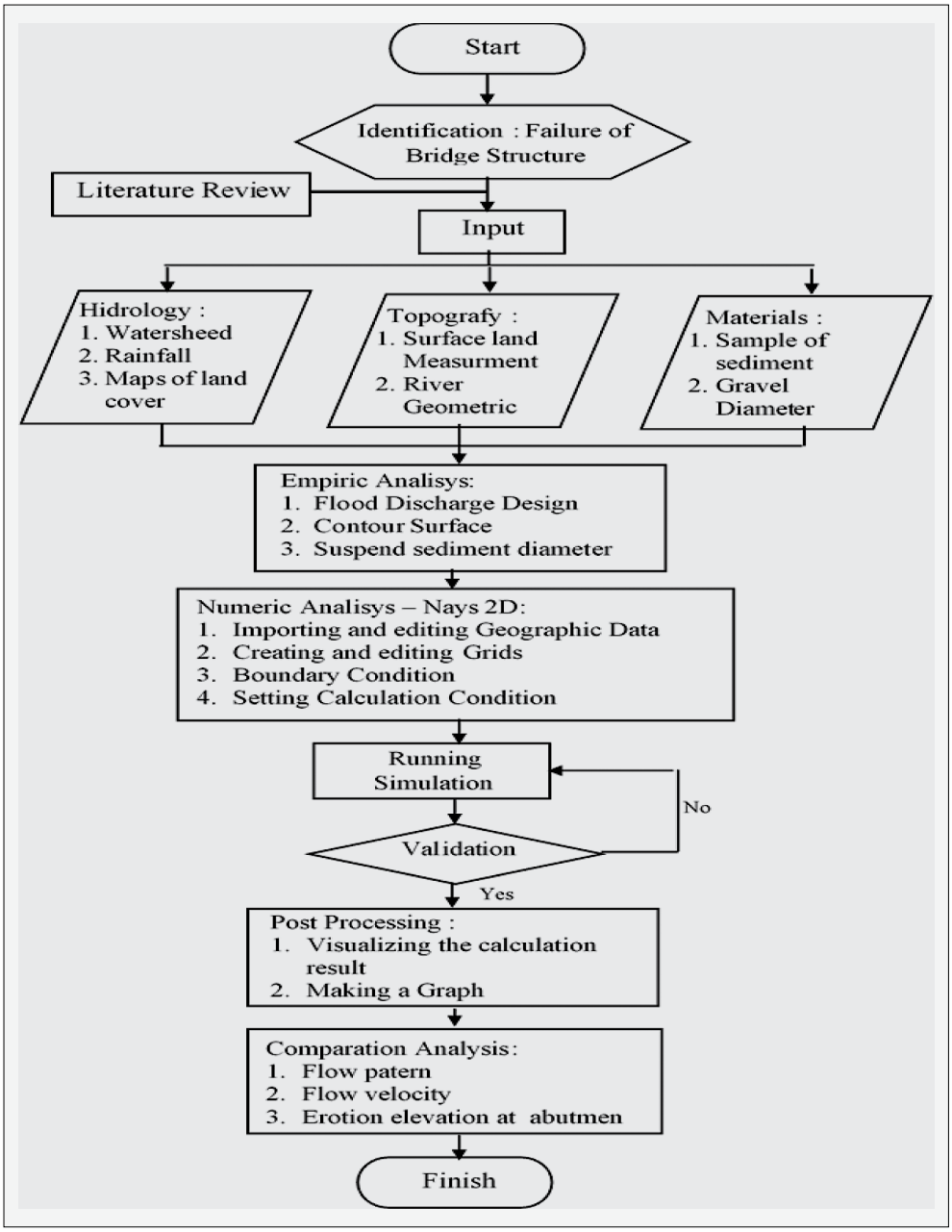

Figure 8: Research flow diagram

2.3. Nays-2DH Simulation

The research was conducted by collecting field measurement data (see **Figure 8**), which were then input into the *iRICNays2DH* application, operated measurement data input with discharges (Q), contour surface, bed roughness, and sediment diameter. Nays2D is a 2D solver used to calculate flow, sediment transport, riverbed evolution, and bank erosion. This solver has been applied to several practical cases, such as the evolution of rivers influenced by vegetation and trees, the calculation and prediction of flood inundation on plain areas, sedimentation at river confluences, as well as analysis of bank erosion and flood disasters (**Ali et al., 2017**).

2.4. Fluid Mass Conservation and Momentum Equation

As we know from the principle of fluid mass conservation, the mass of fluid entering a system is equal to the mass leaving the system. Therefore, before deriving the fluid mass conservation equation, it is necessary to describe the mass balance of a fluid grain, which is the rate of mass of the fluid grain = net rate of mass flow into the fluid element. The rate of mass of the fluid grain can be expressed as follows:

$$\frac{\partial \rho}{\partial t}(\delta x \delta y \delta z) = 0 \tag{5}$$

Where:

ρ = the type of density (kg/m^3),
t = time (s),
$(\delta x \delta y \delta z)$ = the volume of the fluid element (m^3).

Next, we describe the mass flow through the fluid element in a three-dimensional plane, as depicted in the following diagram (see **Figure 6**).

Equation 6 above represents the continuity equation for unsteady fluid flow in three dimensions. However, if we consider, to neglect the vertical component, the equation becomes as follows (see **Figure 7**):

$$\frac{\partial \rho}{\partial t} + \frac{\partial (\rho u)}{\partial x} + \frac{\partial (\rho v)}{\partial y} = 0 \tag{6}$$

with ρ = density (kg/m^3), $u = x$ direction of velocity, $v = y$ and t = time direction of velocity of velocity.

According to Newton's second law, the change in momentum of a fluid grain is equal to the sum of the forces acting on that grain. The change in fluid momentum in the x and y directions can be expressed as follows:

In the x-direction: $$\frac{\partial (\rho v)}{\partial t} + \frac{\partial uv}{\partial x} + \frac{\partial (\rho v^2)}{\partial y} \tag{7}$$

In the y-direction: $$\frac{\partial (\rho u)}{\partial t} + \frac{\partial pu^2}{\partial x} + \frac{\partial (\rho uv)}{\partial y} \tag{8}$$

Equations 7 and **8** represent the momentum change equations where the mass flow rate (kg/s) is multiplied by velocity (m/s). In the *Nays2DH* solver manual, the flow motion is divided into two coordinate systems: the orthogonal coordinate system (x, y) and the *moving boundary fitted coordinates* (MBFC) or linear curve coordinate system (**Takebayashi, 2014**).

3. Results and discussion

The slope of the Harapan watershed (see **Figure 9**) shows a fairly steep slope with a slope of between 12% - 15%, indicating that rainwater has enough time to permeate and become base flow so that surface runoff tends to be small. Precipitation data shows that the average effective rainfall intensity during 3 hours is approximately ± 32.45 mm in wet conditions (see **Figure 10**).

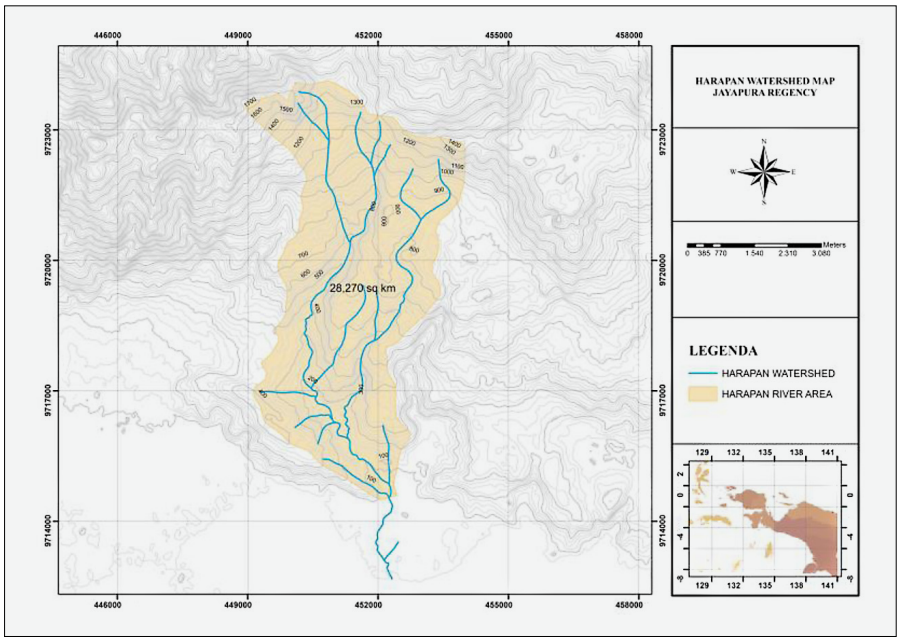

Figure 9: Watershed of Harapan

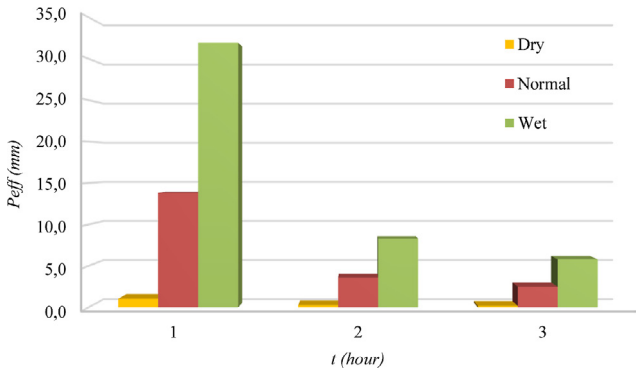

Figure 10: Rainfall Distribution, ABM Method

In this area, there is a big problem since the community carries out sand mining activities around the bridge area and this has a significant impact on changes in river flow and the deposition of sediment brought from upstream. Sand mining also contributes to the widening of the riverbed and leads to sedimentation at specific points that are used for vehicle access (**Sreebha and Padmalal, 2011**). The average cross-section of river and water level can be seen in **Figure 12** and were assessed through sediment sampling conducted using a zigzag pattern up to 1 km from the bridge abutment (see **Figure 11**).

The hydrograph analysis based on equations 1, 2, and 3 indicates the initial and corrected discharge at the peak hour to be 1.83 $m^3/s/mm$ (at a rain depth (h) of 1 mm over the entire watershed area) (see **Figure 13**). Under these specific discharge conditions, the depth of the water surface can be determined as shown in **Figure 12**. Precipitation causes the discharge in the river to rise quickly and causes the catchment area to be large enough, and it allows for rapid surface run-off.

In addition, the rain is projected to persist for a duration of 6 hours, with the most intensity expected within the initial 3 hours following its onset. Subsequently, the flow rate will gradually revert to its usual level by the 6th hour after the rain. The design flood discharge, as shown in **Figure 14**, is the highest possible discharge in

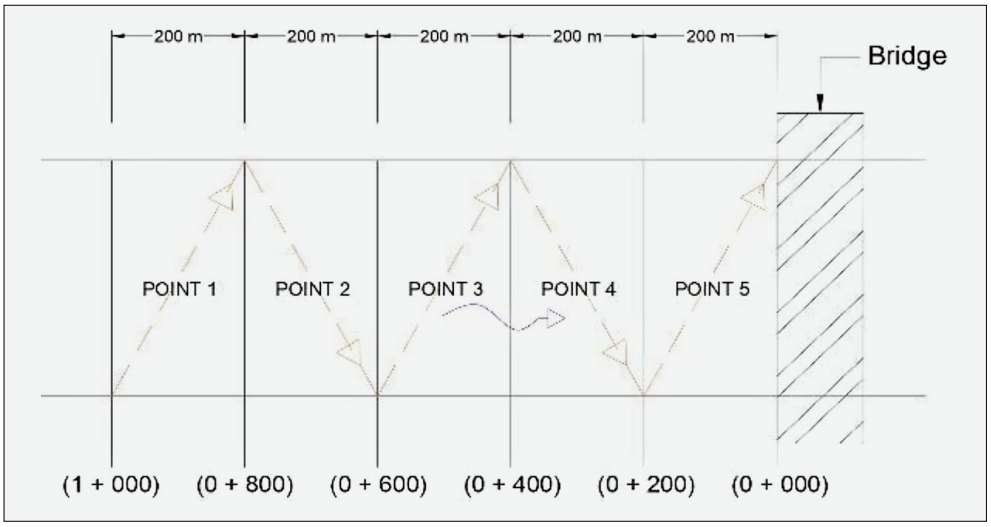

Figure 11: Method of collecting bed material samples

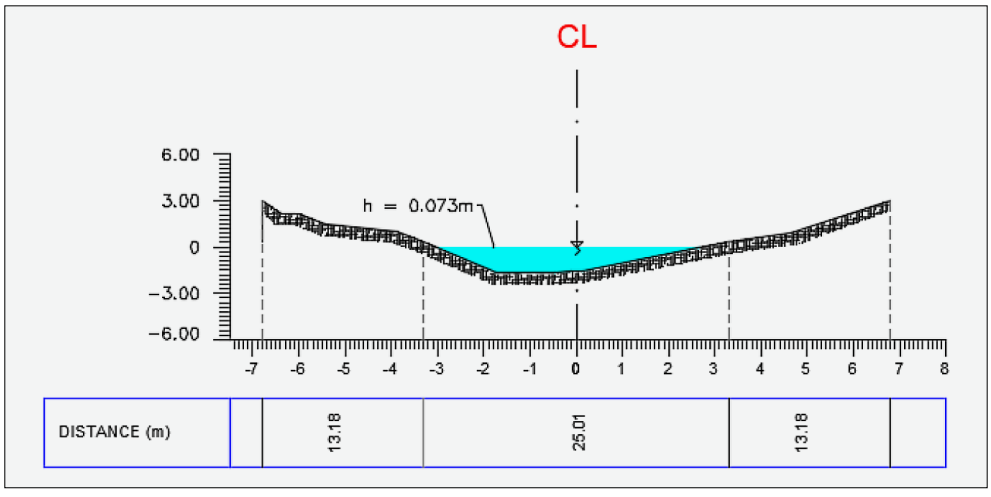

Figure 12: Cross-section river in POINT 1

the river for a specific return period. This discharge results in a peak design flood discharge with a return period of T years, specifically Q_2, Q_5, and Q_{10}, based on the Synthetic Nakayasu hydrograph.

The zigzag sample approach was implemented at the study location, as depicted in **Figure 11** and **Figure 15a**. The riverbed material greatly influences the resistance of the river channel to the force of flowing water, which can cause erosion. The larger the size of the sediment grains, the greater the resistance of the river to erosion. The riverbed material can be transported at a certain flow velocity. The higher the flow velocity, the easier it is for the riverbed material to be transported. This relation can be depicted using the Hjulstrom Curve, which illustrates the zonation of processes occurring in the river cross-section. The classification of flow velocity and sediment size criteria in Harapan River is determined using the *Sturgess* classification method.

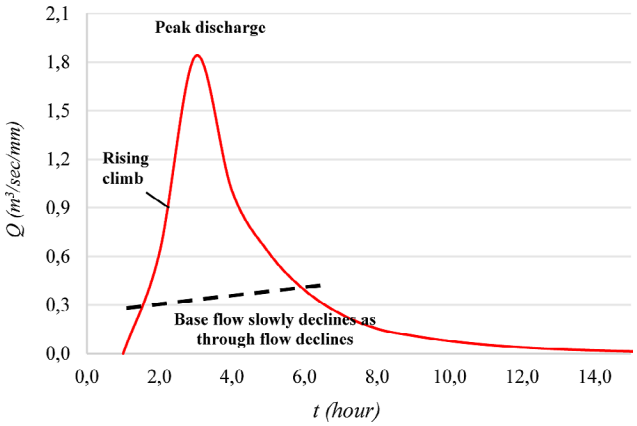

Figure 13: Flood hydrograph at the existing condition

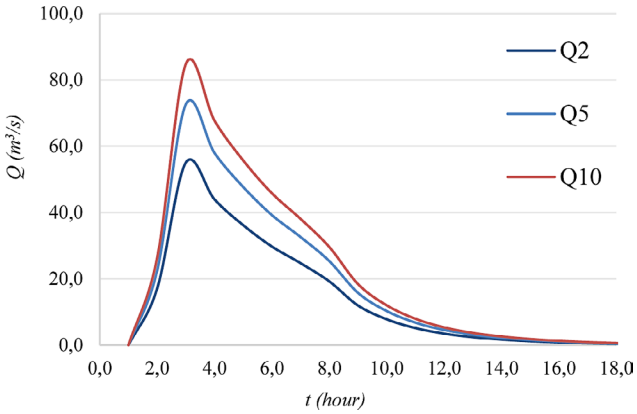

Figure 14: Design flood condition

The average diameter ranges from 14.858 to 20.231 mm, classified as medium gravel to coarse gravel (see **Figure 15b**). The overall diameter size indicates that the average diameter is nearly the same (see **Table 2**) due to being located in the same area with similar sedimentation characteristics. The smallest grain diameter ranges from 4-6.02 mm, while the largest grain diameter ranges from 61.6-70.9 mm. The sediment criteria based on a restrained sieve of 200 with D_{35}, D_{50}, and D_{90} respectively are 0.61 mm, 1.54 mm and 4.52 mm.

Transportation processes occur due to moderate flow velocities (see **Table 3**), allowing the material to move downstream. Location 1 has a small grain of bed material with a diameter of 14.858 mm, and even with a relatively low flow velocity of 99.066 cm/s, it is capable of transporting the bed material at that location. On the other hand, locations 2 and 3 have large-sized grains of bed material, classified as coarse gravel, and low flow velocities. However, despite the low flow velocities, the bed material is already being transported. At point 4, the bed material has an extremely large diameter of 20.231 mm, and the flow velocity is 77.558 cm/s. Under these conditions, the bed material is being transported, but periodic erosion has not yet occurred. At location 5, the flow velocity significantly increases to 352 cm/s due to the proximity to a river bend, and the bed material has a diameter of 19.429 mm. It indicates that the average flow velocity at that location is capable of continuous erosion.

Under the condition of the smallest diameter range (4 - 6.02 mm), almost all locations are above the erosion

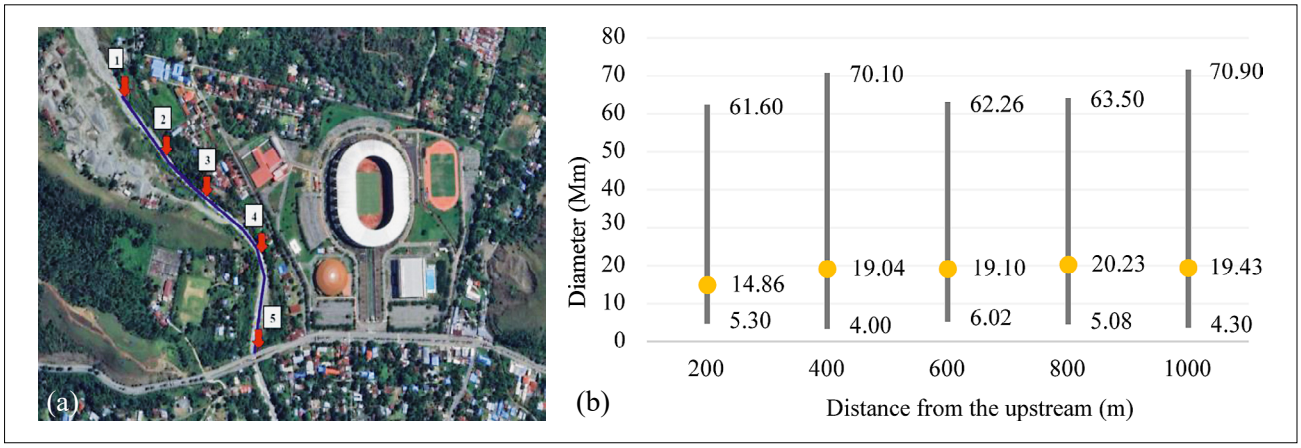

Figure 15: Location point for observation (a) and the graph displays the diameter size of the bed material (b)

velocity threshold, with only one location surpassing the critical velocity threshold at point 4. It indicates that at the minimum diameter condition, the bed material is already being transported and eroded at the same flow velocity. In the case of the largest diameter range (61.6 - 70.9 mm), points 1, 2, and 3 experience the transportation zone. The flow velocity at these points is still capable of transporting the bed material under maximum conditions. At point 4, with a diameter of 63.5 mm, the deposition zone is observed. This condition indicates that the bed material is settling. Point 5 falls into the erosion zone, explaining that the flow velocity at this location is capable of transporting the material, even at the maximum grain size of 70.9 mm. If there is an increase in flow velocity due to a flood, each location can enter the erosion zone on the Hjulstrom Curve and experience erosion.

Table 2: Average grain diameter criteria

Criteria	Average grain diameter (mm)
Small	14.9-16.6
Medium	16.7-18.4
Large	18.5-20.2
Largest	>20.2

Table 3: Average flow velocity criteria

Criteria	Average flows (cm/s)
Small	77.6-160.6
Medium	160.7-243.7
Large	243.8-326.6
Largest	>326.6

3.1 Computational simulation

The velocity and hydraulic structures in the river affect the movement of bed sediments. Placing abutments at river bends has the potential to increase velocity and form vortex flow in the bend area, which can lead to erosion. The eroded material will be deposited on the outer edge of the river and reach the abutment area, potentially causing abutment failure (see **Figure 17a**). To minimize this, the placement of cribs can help reduce flow velocity along the bends before and after the abutment. The cribs are positioned perpendicular to the direction of the river flow, and their alignment follows the longitudinal horizontal line of the river channel. The base of the cribs is placed against the bank to prevent flow from entering behind the cribs, ensuring better stability and resistance against potential landslides. The average flow velocity increases with increasing river discharge; however, by installing cribs, the flow velocity in the river bends can be attenuated and redirected, resulting in lower velocities and better distribution (**Cribs, 2022**).

From the results of running the abutment with the installation of a crib, it can be observed that the magnitude of flow velocity around the abutment decreases, and the flow is well-distributed, resulting in smaller and directed vortices (see **Figure 17b**). When compared to the average velocity in a river equipped with a crib, the resulting changes are not significantly different from the critical velocity of the river. The lowest velocity at each design discharge in the crib area is 1.358 m/s, while the highest velocity at each design discharge in the crib area is 1.835 m/s.

Before entering the abutment, the water experiences significant turbulence with velocities of up to 1.33 m/s. This turbulence does not directly affect the abutment, reducing the risk of erosion on the abutment. When the

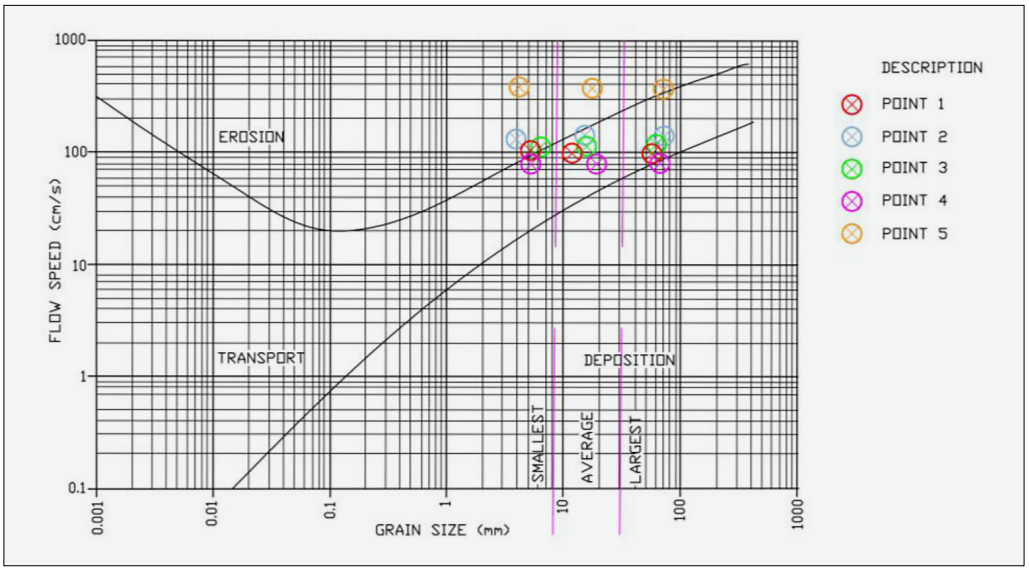

Figure 16: Hjulstrom Curve for the smallest, average, and largest diameter sizes

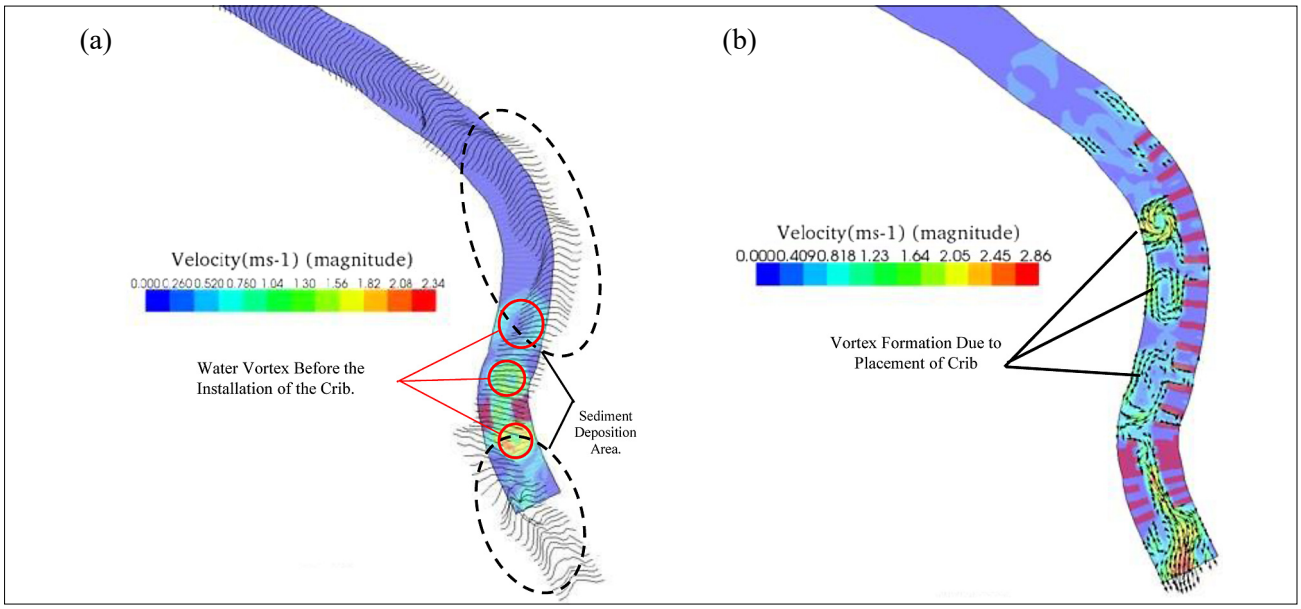

Figure 17: Bedload sediment movement and flow pattern changes at the abutment (a) before the installation of cribs and (b) after the placement of cribs

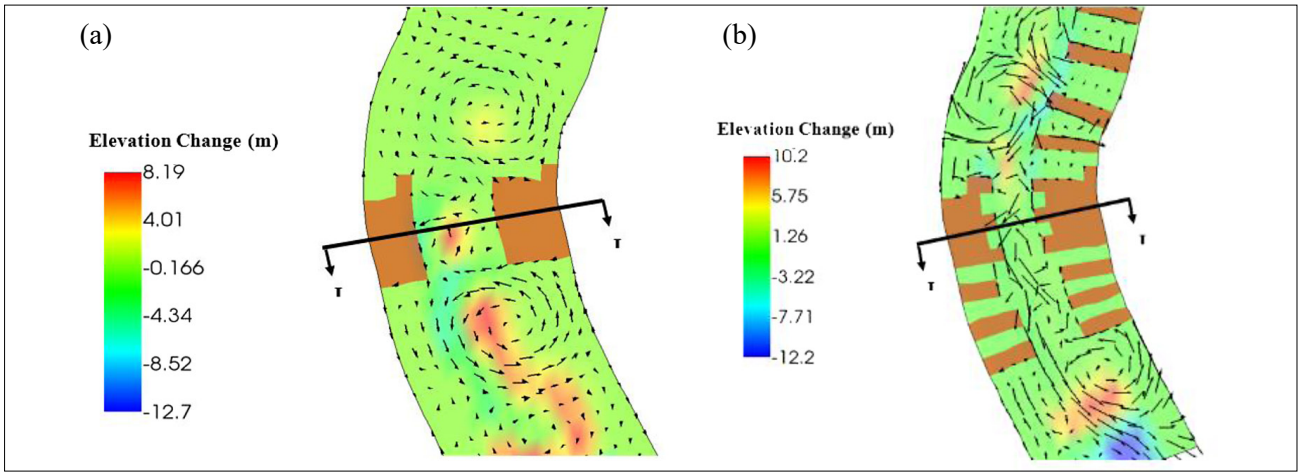

Figure 18: The differences between the pattern of riverbed elevation at the abutment area (a) before the installation of cribs and (b) after the placement of cribs

water flow starts to enter the abutment, the flow velocity direction does not experience turbulence. When the water flow exits the abutment, the flow velocity and river velocity remain stable without any turbulence occurring. The velocity around the abutment does not exceed 1.33 m/s.

The difference in erosion can be observed in the locations where erosion occurs. In the abutment without cribs, erosion occurs directly in contact with the abutment on the right side for each sediment grain diameter. The scour's depth around the abutment is approximately ± -1.50 m and in the middle abutment reaches aggradation up to ± 2.50 m (see **Figure 18a**). As for the aggradation with cribs, it occurs in the middle between the two abutments, with an average depth of ± 1.50 meters for each sediment grain diameter (see **Figure 18b**). On the other hand, in the abutment with cribs, erosion also occurs, but it does not directly contact the abutments. The erosion that occurs is relatively small, except for the sediment grain diameter $D_{50} \approx 1.54$ mm.

As observed in **Figure 19**, the placement of cribs has successfully protected the abutments from erosion on the abutment structure. Degradation of the channel bed still occurs after the installation of cribs; however, this degradation does not affect the abutment structure itself. The cribs prevent and safeguard the abutments from the erosion of the riverbed.

4. Conclusions

According to the analysis, it seems that sediment movement is influenced by the existing flow speed of

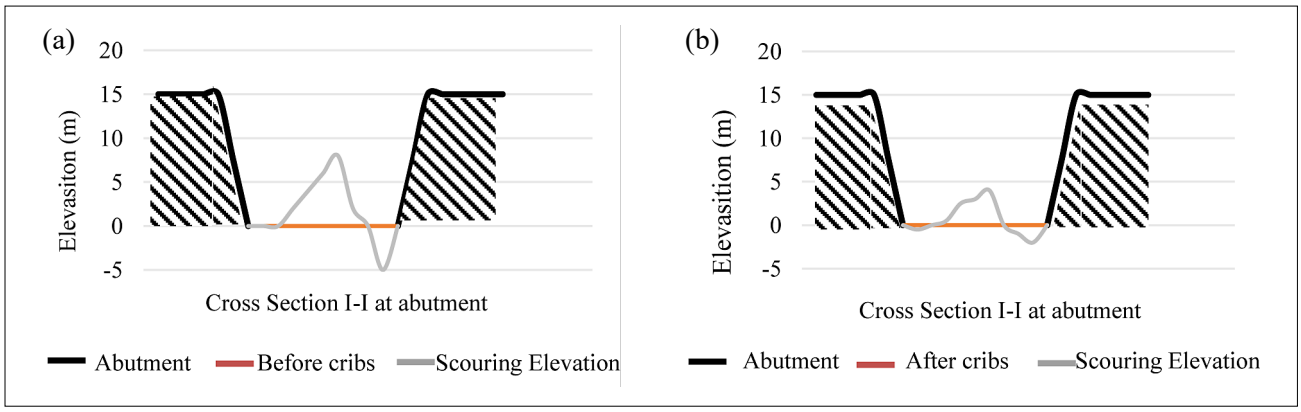

Figure 19: Bed change elevation profile at the abutment area
(a) before the installation of cribs and (b) after the placement of cribs

1.33 m/s, which is able to lift and shift little silt that meets certain criteria. This condition will affect how sediment moves along the river. If flood conditions arise with a specific recurrence interval, there is a possibility of experiencing more substantial harm to infrastructure. An investigation of the sediment motion stability around bridge abutments before and after the installation of cribs in order to prevent structural failures has been done. The bed material grain characteristics in Harapan River fall within the category of medium gravel to *coarse gravel*, as defined by the *American Geophysical Union*, with an average diameter ranging from 14.85 to 20.23 mm. The placement of cribs in the curved sections, both upstream and downstream of the abutments, effectively directs and slows down the flow velocity. Consequently, the velocity changes around the abutments are reduced, leading to a well-distributed flow pattern characterized by smaller and directed vortexes. Moreover, the cribs regulate elevation changes in the riverbed, including both aggradation and degradation, based on planned placement. Furthermore, the cribs serve as protection against the risk of erosion around the abutment structure.

5. References

Abdelaziz, A., & Lim, S. (2017): Scour hole characteristics around abutment in compound channel. 389–401. doi: 10.1061/9780784480625.036.

Ali, M. S., Hasan, M. M., & Haque, M. (2017): Two-dimensional simulation of flows in an open channel with groin-like structures by iRIC Nays2DH. *Mathematical Problems in Engineering*, *2017*. doi: 10.1155/2017/1275498

Armenio, V. (2017): Large eddy simulation in hydraulic engineering: Examples of laboratory-scale numerical experiments. *Journal of Hydraulic Engineering*, *143*(11), 031 17007. doi: 10.1061/(asce)hy.1943-7900.0001357

Ballio, F., Radice, A., & Dey, S. (2010): Temporal scales for live-bed scour at abutments. *Journal of Hydraulic Engineering*, *136*(7), 395–402. doi: 10.1061/(asce)hy.1943-7900.0000191

Ballio, F., Teruzzi, A., & Radice, A. (2009): Constriction effects in clear-water scour at abutments. *Journal of Hydraulic Engineering*, *135*(2), 140–145. doi: 10.1061/(asce)0733-9429(2009)135:2(140)

Choi, H.-K., Baek, K.-W., & Choi, Y.-M. (1999): A Study on Proposal of Appropriate Rainfall-Runoff Model With Watershed Characteristics. *Journal of Industrial Technology*, *19*, 379–390

CRIBS, E. B. I. I. (2022): Modeling The Control Of River Bend Bed Erosion By Installing Impermeable Cribs. *Journal of Engineering Science and Technology*, *17*(5), 3489–3511.

Hong, S. H., Sturm, T. W., & Stoesser, T. (2015): Clear water abutment scours in a compound channel for extreme hydrologic events – *Journal of Hydraulic Engineering*, *141*(6), 04015005. doi: 10.1061/(asce)hy.1943-7900.0001002

Koken, M., & Constantinescu, G. (2014): Flow and turbulence structure around abutments with sloped sidewalls. *Journal of Hydraulic Engineering*, *140*(7), 04014031. https://doi.org/10.1061/(ASCE)HY.1943-7900.0000876

Lerche, D. (2019): Comprehensive characterization of nano- and microparticles by in-situ visualization of particle movement using advanced sedimentation techniques. *KONA Powder and Particle Journal*, *36*, 156–186. https://doi.org/10.14356/kona.2019012

Geier T.W, "To Aid in Securing Favorable Conditions of Water Flows Applied River Morphology," no. October, 1996, [Online]. Available https://search.yahoo.com/search?fr=mcafee&type=E210US885G0&p=Gregory+S.+Bevenger+and+Rudy+M.+King%2C+1995%2C+A+Pebble+Count+Procedure+for+Assessing+Watershed+Cumulative+Effects. (accessed September 21st, 2023)

Nelson, J. M., Bennett, J. P., & Wiele, S. M. (2003): Flow and sediment-transport modeling. *Tools in Fluvial Geomorphology*, *18*, 539–576.

Radice, A., Ballio, F., & Porta, G. (2009): Local scour at a trapezoidal abutment: Sediment motion pattern. *Journal of Hydraulic Research*, *47*(2), 250–262. doi: 10.3826/jhr.2009.3356

Radice, A., & Davari, V. (2014): Roughening elements as abutment scour countermeasures. *Journal of Hydraulic*

Engineering, *140*(8), 06014014. doi: 10.1061/(asce)hy.1943-7900.0000892

Shahsavari, H., Heidarpour, M., & Mohammadalizadeh, M. (2017): Simultaneous Effect Of Collar And Roughness On Reducing And Controlling The Local Scour Around Bridge Abutment. *Acta Universitatis Agriculturae et Silviculturae Mendelianae Brunensis*, *65*(2). doi: 10.11118/actaun201765020491

Sreebha, S., & Padmalal, D. (2011): Environmental impact assessment of sand mining from the small catchment rivers in the southwestern coast of India: A case study. *Environmental Management*, *47*, 130–140. https://doi.org/10.1007/s00267-010-9571-6

Takebayashi, Y. A. H. (2014): iRIC Software Nays2DH Solver Manual. 1–64p

Widyastuti, I., Thaha, M. A., Lopa, R. T., & Hatta, M. P. (2022): Dam-break energy of porous structure for scour countermeasure at bridge abutment. *Civ. Eng. J*, *8*(12), 3939–3951. doi: 10.28991/CEJ-2022-08-12-019

SAŽETAK

Simulacija utjecaja montažne konstrukcije na kretanje riječnoga sedimenta uz upornjak mosta (studija slučaja: rijeka Harapan, regija Jayapura)

Erozija nastaje kada brzina tijeka u kanalu premaši graničnu brzinu koja uzrokuje pomicanje nataloženoga sedimenta. Ovaj se fenomen opaža u rijeci Harapan, što rezultira spuštanjem i sužavanjem riječnoga korita u dijelu gdje se nalaze potporne konstrukcije (upornjak mosta). Cilj je ovoga istraživanja istražiti stabilnost sedimenta oko upornjaka mosta prije i nakon ugradnje montažnoga potpornog zida kako bi se spriječili strukturni slomovi upornjaka mosta. Uzorkovanje sedimenta provedeno je na šest točaka oko upornjaka mosta, metodom brojenja valutica (eng. *Pebble Count Method*) duž cik-cak putanja. Veličina zrna sedimenta klasificirana je prema klasifikaciji Sturgess, a proces disperzije materijala analiziran je pomoću Hjustormove krivulje. Projektna vrijednost količine oborina predstavlja protok koji bi bio posljedica poplave, koji je zatim simuliran korištenjem dvodimenzionalne hidrodinamike, analizirajući uvjete u rijeci prije i nakon postavljanja montažnoga potpornog zida. U slučaju bez montažne potporne konstrukcije erozija sedimenta javlja se uz upornjak na desnoj strani riječnoga korita. Erozijom su zahvaćeni svi promatrani promjeri zrna nataloženoga sedimenta. U slučaju kada je postavljena montažna potporna konstrukcija, erozija je i dalje prisutna, ali ne neposredno uz samu konstrukciju upornjaka. Montažni potporni zid osigurao je stabilnost upornjaka mosta smanjujući eroziju riječnoga korita.

Ključne riječi:
2D simulacija, montažni potporni zid, rijeka Harapan, dinamička stabilnost riječnoga sedimenta

Author's contribution

Ira Widyastuti (1) (Lecturer, hydrology) conceptualization methodology, review editing, project administration, and writing the original draft**. Mujiati (2)** (Lecturer, civil engineering) data analysis, and computational analysing. **Davy Ivan Robert Jansen (3)** (Lecturer, hydraulic) data analysing, conceptualization, and writing the original draft. **Ahmad Fauzi Yunus (4)** (Researcher, civil engineering) writing the original draft, and sediment analysis.